DOI: 10.15415/jnp.2016.32021

Effects of Aging Time and Sintering Temperatures on Thermal, Structural and Morphological Properties of Coralline Hydroxyapatite

MANINDER SINGH MEHTA[1] AND RAVINDER PAL SINGH[2]

[1,2]Department of Mechanical Engineering, Sri Guru Granth Sahib World University, Fatehgarh Sahib, Punjab, India

Email: mehtadiary@gmail.com

Received: October 10, 2015 |Revised: January 08, 2016 |Accepted: January 08, 2016

Published online: February 08, 2016, The Author(s) 2016. This article is published with open access at www.chitkara.edu.in/publications

Abstract: Biphasic Calcium Phosphate bioceramics belong to a group of bone substitute biomaterials comprised of an intimate mixture of Hydroxyapatite (HAP) and β-Tricalcium Phosphates. In the present work, Coralline Hydroxyapatite was synthesized using wet precipitation method. Powder particles were aged for 24 and 48 hours at 5. X-Ray Diffraction, Fourier Transform Infrared and Thermogravimetric spectroscopic techniques were used. Biphasic Calcium Phosphate was identified as the chief structural constitution of the synthetic powders. Weight fraction of Hydroxyapatite increased with the rise of sintering temperature. Aging time of 24 hours yielded maximum amount of hydroxyapatite, thus confirming optimum aging time for the synthesis of Coralline Hydroxyapatite.

Keywords: HAP, Corals, Aging Time, Sintering Temperature, BCP.

1. INTRODUCTION

HAP [$Ca_{10}(PO_4)_6(OH)_2$] is the dominant inorganic phase in natural bone. HAP is widely used in the biomedical field because of excellent biocompatibility, high bioactivity, non-toxicity, non-inflammatory behavior and non-immunogenic properties. HAP has rapid bone regeneration ability and creates a direct bond with the host living bone without intermediate connective tissue [1]. Such capabilities have made HAP an ideal candidate for orthopedic and dental implants. Among the various factors critically affecting the biological response to the implant material include structural constitution of synthetic particles, their morphology and spread etc [2]. Such inherent properties exclusively depend upon the type of adopted synthesis protocol and its allied process parameters.

Journal of Nuclear Physics, Material Sciences, Radiation and Applications
Vol-3, No-2
Feburary 2016
pp. 223–237

CHITKARA UNIVERSITY

In the present study, wet precipitation synthesis of HAP from easily and cheaply available corals has been presented.In addition, effects of various process parameters viz. aging time and sintering temperatures on the intrinsic properties of coralline HAP (C-HAP) were also analyzed comprehensively.

2. MATERIALS AND METHODOLOGY

2.1. Materials

Gonipora corals and di-calcium phosphate (Merck, 99%) were used as a calcium and phosphorous ion sources throughout. Double distilled water was used as a solvent.

2.2. Synthesis Methodology

Adopted synthesis methodology has been comprehensively elaborated in Fig 1.

2.3. Characterization Techniques

X-Ray Diffraction (Philips X'Pert 1710) analysis was performed for all powders using CuKα radiation (λ= 1.54 Å, 2= 10 to 80, step size 0.017, time per step 20.03 s and scan speed 0.005/s). Relative amount of different phases present were estimated on the basis of the peak intensity variation by means of external standard method. Lattice parameters were calculated using Equation 1:

$$\frac{1}{d^2} = \frac{4}{3}\left\{\frac{h^2 + hk + k^2}{a^2}\right\} + \frac{l^2}{c^2} \qquad \text{(Eq. 1)}$$

where d is the distance between adjacent planes in the set of Miller indices (hkl),the reference for HAP being JCPDS file no. 09-0432 (a=9.418Å, b=9.418 Å, c=6.884 Å, space group p63/m) and for TCP being JCPDS file no. 01-070-0364 respectively. Crystallite size was calculated using Scherrer's Equation 2:

$$X_s = \frac{0.9\lambda}{\beta Cos\square} \qquad \text{(Eq. 2)}$$

whereX_s is the crystallite size in nanometer, λ is the wave length of x-ray beam, β is the broadening of diffraction line at half of its maximum intensity in radians, and is the Bragg's diffraction angle ().

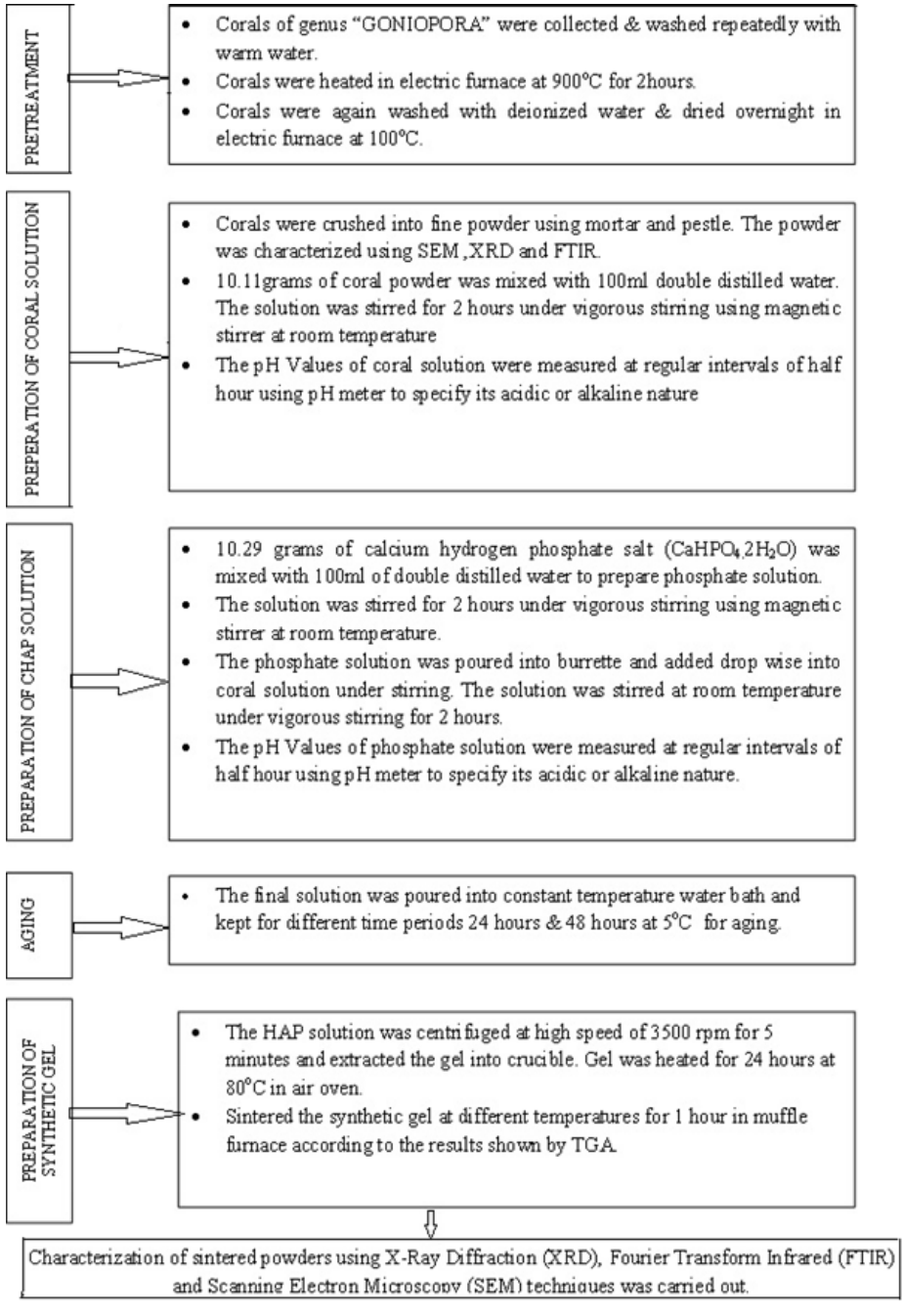

Figure 1: Synthesis Methodology.

The relative amounts of HAP and β-TCP in the synthesized powder were determined using external standard method as given in Equation 3.

$$\frac{I_{\beta TCP(0210)}}{I_{HAP(211)}} = \frac{\text{Weight of} \beta - TCP}{\text{Weight of HAP}} \quad \text{(Eq. 3)}$$

where $I_{\beta\text{-TCP}(0210)}$ is the intensity of β-TCP peak having (0 2 1 0) as (h k l) plane and I_{HAP} is the intensity of HAP peak having (2 1 1) as (h k l) plane respectively.

Calcium deficiency (x) of synthetic HAP powder was calculated by converting the weight ratio into molar ratio as follows:

$$\frac{Mol_{\beta TCP}}{Mol_{HAP}} = \frac{Wt_{\beta TCP}}{Wt_{HAP}} x3.23 \quad \text{(Eq. 4)}$$

$$\frac{Mol_{\beta TCP}}{Mol_{HAP}} = \frac{3x}{1-x} \quad \text{(Eq. 5)}$$

Where x is a calcium deficiency of synthesized powder.

Calcium to phosphorous (Ca/P) ratio was further calculated using Equation 6 as follows:

$$\frac{Ca}{p} = \frac{10-x}{6} \quad \text{(Eq. 6)}$$

Thermal behavior of as-synthesized gel was investigated using Thermogravimetry (TGA, Perkin Elmer STA 6000), with an accuracy of ±0.1 μg in weight measurement and ±0.5C in temperature measurement. All the tests were performed in air environment under the following conditions: heating rate 5C/min, peak temperature 1000C and air flow 20.0 mL/min.

Infrared spectra (FTIR Perkin Elmer) were recorded in the region 400-4000 cm^{-1} using KBr pellets (1% wt/wt), with spectral resolution of 2 cm^{-1}, taking four scans for each sample.

Morphology of synthetic powders was observed using Scanning Electron Microscopy (SEM, JEOL); operated at a voltage of 15 kV.

3. RESULTS AND DISCUSSION

3.1. Raw

Corance of Calcium Carbonate ($CaCO_3$) and Calcium Oxide (CaO) as the only constituentphases [Mehta et al. (2014)].Weight fraction of $CaCO_3$was observed to be 99%, whereas CaO was present in traces i.e. ~1%. No other phase was observed.

3.1.2. FTIR Analysis

Small and narrow peak at 3640 cm^{-1}(Fig 3) reveals the presence of OH functional group, thus disclosed the presence of water adsorption deformation functional group in the raw coralline powder [17]. Clustered peaks between 400-500 cm^{-1} was considered as the background disturbance of equipment and hence neglected.

Thus analysis of XRD and FTIR results concluded $CaCO_3$ and CaO as the primary compounds, whereas OH was detected as the only constituent ionic group comprising the corals. Hence, selected corals were considered as the rich source of calcium (Ca) ions, thus suitable for the production of HAP or other allied phases of Calcium Phosphate (CaP) family.

3.2. C-HAP

C-HAP powder was synthesized at different aging times (24 hours and 48 hours) at a controlled aging temperature of 5. Synthesized powders were sintered at different temperatures as depicted by TG analysis. Six powders were prepared, categorized and nomenclature on the basis of their respective aging time and sintering temperatures as shown in Table 1.

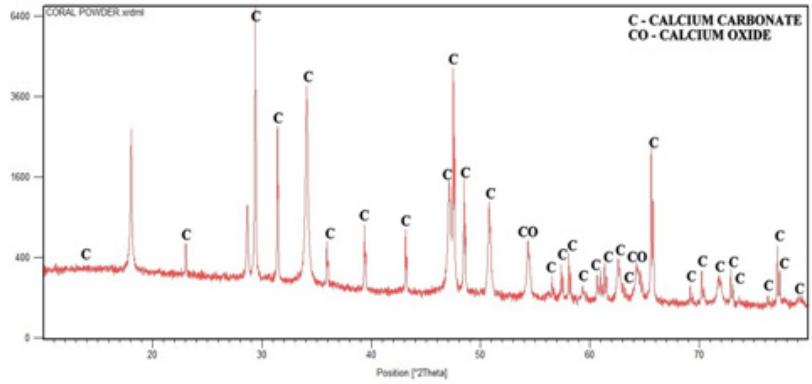

Figure 2: XRD of Raw Coralline Powder

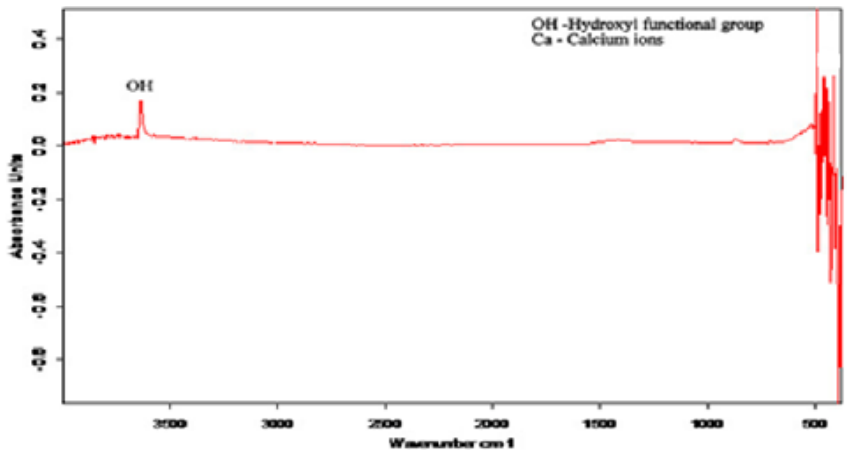

Figure 3: FTIR of Raw Coral Powder.

Table 1: Nomenclature on the Basis of Aging Time and Sintering Temperatures.

S. No.	Powder Nomenclature	Aging Time	Sintering Temperature
1	C-HAP-24-415	24 Hours	415°C
2	C-HAP-24-533	24 Hours	533°C
3	C-HAP-24-790	24 Hours	790°C
4	C-HAP-48-400	48 Hours	400°C
5	C-HAP-48-520	48 Hours	520°C
8	C-HAP-48-800	48 Hours	800°C

3.2.1. TG Analysis

TGA of as preparedC-HAP gel synthesized after an aging time of 24 hours (Fig 4) suggested three distinct phase transformation regions. Three different temperatures viz. 415°C, 533°C and 790°Cwere chosen where mass change was observed to be maximum. Thus respective C-HAP gel was further sintered at 415°C, 533°C and 790°C respectively and characterized for their structural and morphological transformations.

As prepared C-HAP gel synthesized after an aging time of 48 hours was also tested for its thermodynamic analysis and results have been depicted in Fig 5.Three distinct phase transformation regions were observed suggesting 400°C, 520°C and 800°C temperatures at which mass change of respective

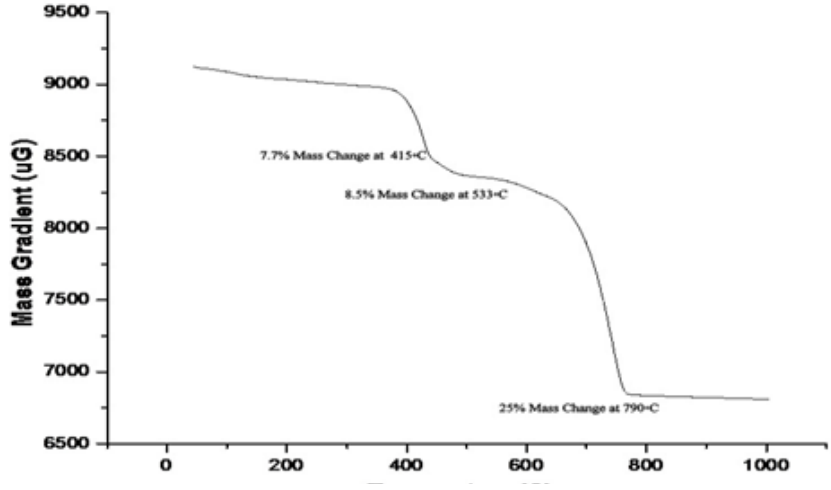

Figure 4: Thermogramof C-HAP Powder Prepared after anAging Time of 24 Hours.

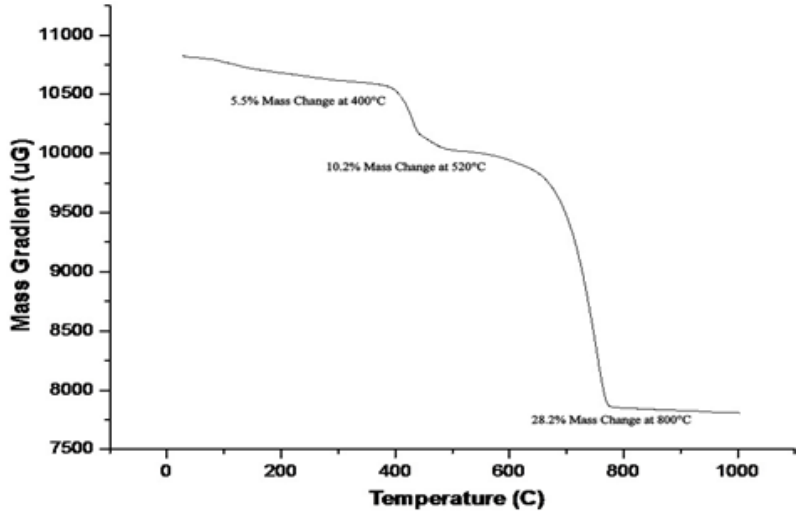

Figure 5: L Thermogram of C-HAP Powder Prepared after anAging Time of 48 Hours.

C-HAP powder was observed to be affected maximally. Therefore, taking care of TGA interpretation respective C-HAP gel was further sintered at 400°C, 520°C and 800°C and obtained powders were further characterized for their structural and morphological transformations.

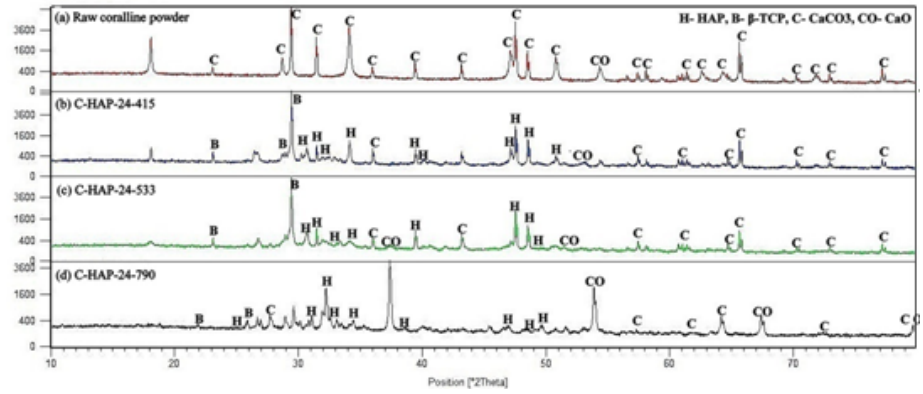

Figure 6: Diffractograms of (a) Raw coralline powder, (b) C-HAP-24-415, (c) C-HAP-24-533 and (d) C-HAP-24-790Powders.

Table 2: Calculated Structural Properties of 24 Hours Aged C-HAP Powders.

	C-HAP-24-415	C-HAP-24-533	C-HAP-24-790
Phases	HAP, β-TCP, $CaCO_3$, CaO	HAP, β-TCP, $CaCO_3$, CaO	HAP, β-TCP, $CaCO_3$, CaO
HAP Lattice Parameters	a = 9.507nm, c=6.882nm, c/a=0.724	a = 9.525nm, c=6.890nm, a=0.723	a = 9.386nm, c=6.892nm, c/a=0.734
HAP Mean Crystalline Size	76.04 nm	79.57 nm	82.85 nm
Weight %age	HAP=28.44%, β-TCP=50.81% $CaCO_3$=20.07% CaO=0.68%	HAP=39.69% β-TCP=14.25% $CaCO_3$=43.48% CaO=2.58%	HAP=45.99% β-TCP=21.70% $CaCO_3$ = 9.31% CaO=23.66%
Calcium Deficiency(x)	0.65	0.27	0.33
Ca/P	1.56	1.62	1.61

3.2.2. XRD Analysis

X-Ray diffractograms of raw coralline and sintered C-HAP powders (aging time of 24 hours) have been shown in Fig 6. Diffractograms disclosed the multiphasic constitution of synthesized powders. $CaCO_3$, HAP and β-Tricalcium Phosphate (β-TCP) were the primary structural compositions throughout all the powders[17].$CaCO_3$ and CaO impurities were also present in various proportions. Narrow and sharp peaks indicated the big and crystalline crystal structure of synthesized powders.

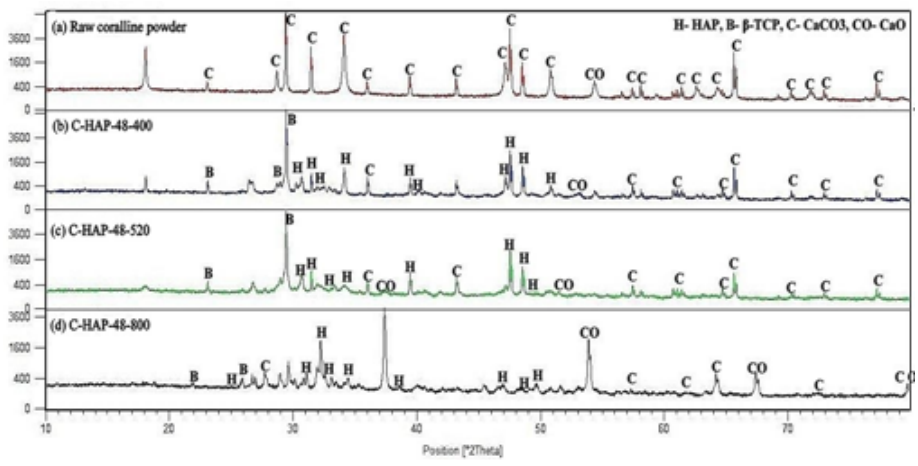

Figure 7: Diffractograms of (a) Raw coralline powder, (b) C-HAP-48-400, (c) C-HAP-48-520 and (d) C-HAP-48-800Powders.

Various structural properties were calculated and have been enumerated in Table 2 which disclosed that crystallite size and weight percentage of HAP phase increased with the rise of sintering temperature [17]. Lattice parameters and their distortion (c/a ratio) also varied with the change of sintering temperature. Calcium deficiency (x) decreased, whereas Ca/P ratio of synthetic powders increased with the rise of temperature. Ca/P ratio varied between 1.5-1.66, which confirmed the existence of calcium deficient HAP powder.

XRD diffractograms of raw coralline and sintered C-HAP powders prepared at an aging time of 48 hours have been shown in Fig 7. Multiphasic chemical constitution primarily composed of HAP, β-TCP and $CaCO_3$ were identified. CaO was present in traces. Narrow, sharp and distinct peaks represented large and crystalline phases respectively. Similar trend of increase of HAP %age was noticed with the rise of sintering temperature.

As expected, lattice parameters and crystalline size of HAP phase increased with the rise of sintering temperature. HAP percentage also increased with the rise of sintering temperature as shown in Table 3. Sintering temperature also caused the HAP percentage to increase due to the decrease of calcium deficiency (x).Consequently, Ca/P ratio increased and was found to be very close to the stoichiometric value of 1.67 [17].

Comparison of XRD results concluded that phase constitution was remained same, thus having negligible effects of aging time and sintering temperatures on their phase constitution. But, various other structural properties viz. HAP crystallite size, weight %age, calcium deficiency and consequent Ca/P ratio

Table 3: Calculated Structural Properties of 48 Hours Aged C-HAP Powders.

	C-HAP-24-415	C-HAP-24-533	C-HAP-24-790
Phases	HAP, β-TCP, $CaCO_3$, CaO	HAP, β-TCP, $CaCO_3$, CaO	HAP, β-TCP, $CaCO_3$, CaO
HAP Lattice Parameters	a = 9.507nm, c=6.882nm, c/a=0.724	a = 9.525nm, c=6.890nm, a=0.723	a = 9.386nm, c=6.892nm, c/a=0.734
HAP Mean Crystalline Size	76.04 nm	79.57 nm	82.85 nm
Weight %age	HAP=28.44%, β-TCP=50.81% $CaCO_3$=20.07% CaO=0.68%	HAP=39.69% β-TCP=14.25% $CaCO_3$=43.48% CaO=2.58%	HAP=45.99% β-TCP=21.70% $CaCO_3$=9.31% CaO=23.66%
Calcium Deficiency(x)	0.65	0.27	0.33
Ca/P	1.56	1.62	1.61

were compared to differ at different aging times. Mean crystallite size of HAP phase was smaller in case of 24 hour aged powders as expected.Similarly, weight fraction of HAP phase was observed to be more at an aging time of 24 hours.

3.2.3. FTIR Analysis

Presence of functional groups in synthesized powders was detectedby using FTIR analysis and corresponding results have been shown in Fig 8-9.

Fig 8 corresponding to 24 hours aged C-HAP powders revealed the existence of ν_5 P-O(H) deformation of HPO_4^{-2} corresponding to 876 cm^{-1} sharp peak, $\nu_3(PO_4)$ corresponding to broad band stretched from 993-1116 cm^{-1} and carbonate stretching band given by 1328-1559 cm^{-1}.With the rise of sintering temperature,intensity of ν_5 P-O(H) deformation of $HPO_4^{-2}$and carbonate stretching band decreased and ultimately vanished at a sintering temperature of 790°C.On the other hand, peak corresponding to $\nu_3(PO_4)$ ionic group became narrower and deep showing its increase of crystallinity.XRD analysis also supported the increase of crystallinity with the rise of sintering temperature. Noise as present in FTIRs (Fig 8) was neglected. Carbonate ions might have come from the atmosphere, while preparing the solution/powder which completely disappeared with the rise of sintering temperature. On the other hand, PO_4 functional group remained intact with the rise of sintering temperature, thus supported the formation of PO_4 based product. Presence of PO_4ion at the 415°C supports the existence of HAP phaseand also supports the XRD analysis [17].

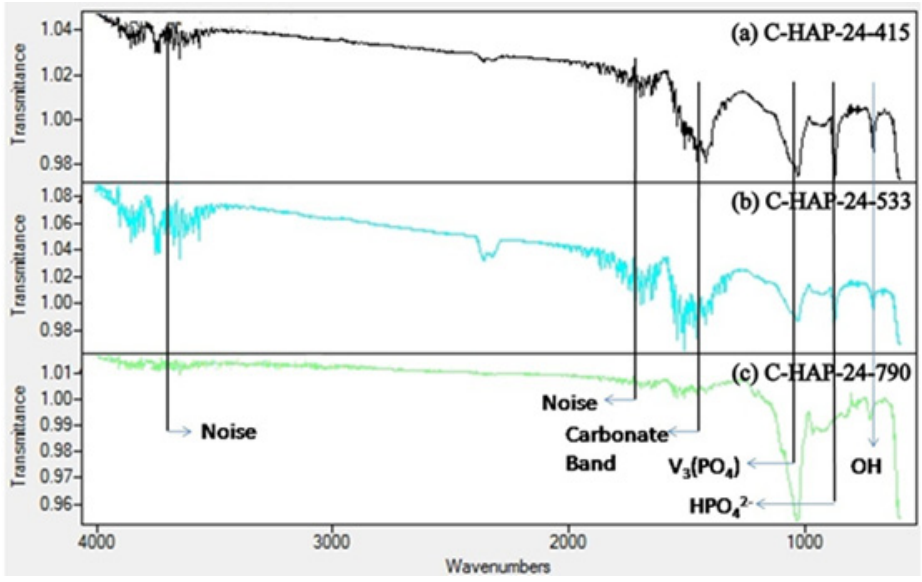

Figure 8: FTIR Analysis of C-HAP Powders Synthesized at Aging Time of 24 Hoursand Sintered at (a) 415°C, (b) 533°C and (c) 790°C.

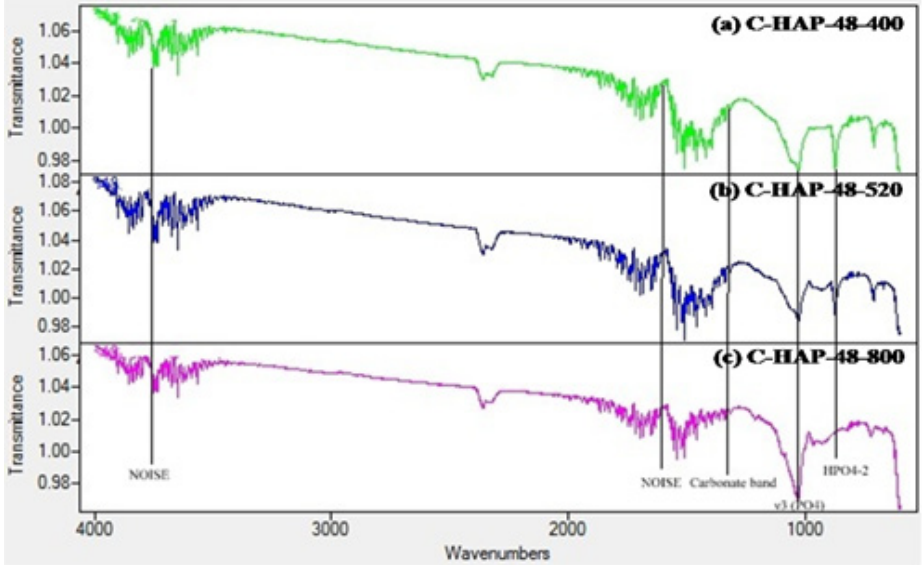

Figure 9: FTIR Analysis of C-HAP Powders Synthesized at Aging Time of 48 Hoursand Sintered at (a) 400°C, (b) 520°C and (c) 800°C.

Fig 9 showingFTIRs of 48 hours aged C-HAP powders revealed the existence of ν_5 P-O(H) deformation of HPO_4^{-2} corresponding to sharp peak at 873 cm^{-1}, ν_3 (PO_4) corresponding to broad band stretched from 1002-1100 cm^{-1} and carbonate stretching band given by 1338-1565 cm^{-1}.With the rise of sintering temperature,intensity of ν_5 P-O(H) deformation of HPO_4^{-2}decreased and ultimately vanished at a sintering temperature of 800°C.On the other hand, peaks corresponding to ν_3 (PO_4) and carbonate stretch became narrower showing increase of their crystallinity.XRD analysis also supported the increase of crystallinity with the rise of sintering temperature. Noise was neglected. Carbonate ions might have come from the atmosphere, while preparing the solution/powder. On the other hand, PO_4 functional group remained intact with the rise of sintering temperature thus supported the formation of PO_4 based product.

Comparison of FTIR results concluded the presence of lesser impurities viz. carbonate and HPO_4 in powders aged at 24 hours at higher temperatures. Except this outcome, ionic constitution remained similar and intact to each other.

3.2.4. SEM Analysis

Particle morphology of powders prepared at 24 and 48 hours aging times, each sintered at 800 have been shown in Fig10-11 respectively.

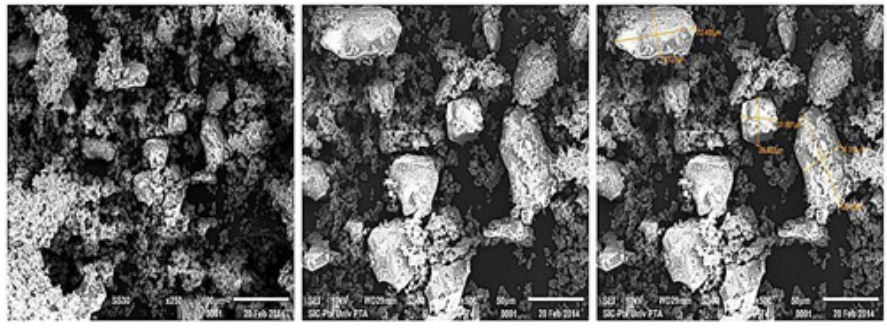

Figure 10: SEM of C-HAP Powder Aged for 24 Hours and Sintered at 790 at various magnifications.

Fig 10-11 revealed the loose, unagglomerated mixture of particles having vivid particle shapes and sizes ranging from very small to large having 1.669-72.488 µm respectively. Aspect ratio of particles was averaged to be 1.558 with mean roundness of 0.889.

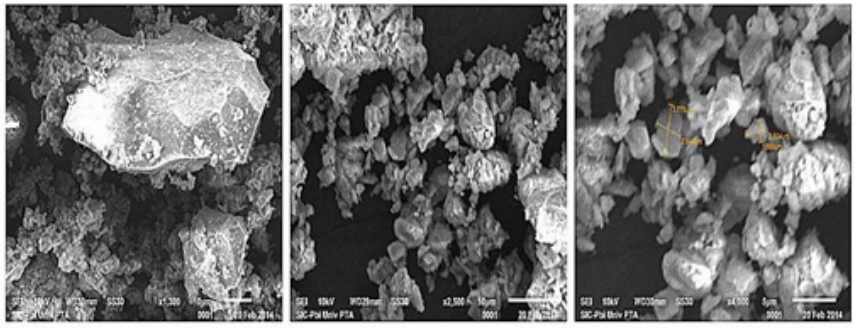

Figure 11: SEM of C-HAP Powder Aged for 48 Hours and Sintered at 800 at various magnifications.

CONCLUSION

The present study detailed the methodology to prepare the C-HAP powder using wet precipitation method. In addition, effects of aging time and sintering temperatures on various properties of synthetic powders were also studied. Results comparison demonstrated that aging time of 24 hours was observed to be optimum in view of presence of more weight percentage of HAP phase with lesser impurities as revealed from XRD and FTIR analysis. Except this outcome, thermal behavior and powder morphology were found to be similar to each other. On the other hand, sintering temperature was noted to influence the structural properties significantly. Weight percentage of HAP phase increased with the increase of sintering temperature and it affected calcium deficiency and Ca/P ratio of synthetic powders. Ionic constitution was also prone to alterations subjected to change of sintering temperatures. In nutshell, aging time of 24 hours and sintering temperature near to 800 were concluded to be the optimum process parameters to prepare C-HAP powders.

REFERENCES

[1] Adamopoulous, E.I, Potaridis, K, (2007). A novel computational method to quantify and analyseosteoclastic bone resorption, Journal of computational methods in science and engineering, pp. 87-91.

[2] Ahmed, S, Ahsana, M, (2008). Synthesis of Ca-hydroxyapatite Bioceramic from Egg Shell and its Characterization,Bangladesh J. Sci. Ind. Res, **43**, pp. 501-512.

[3] Ajie, H, Kaplan, I. R, Slota, P.J, Taylor, R.E, (1990). AMS radiocarbon dating of bone osteocalcin. Nuclear Instruments and Methods, **52**, pp. 433-437. http://dx.doi.org/10.1016/0168-583X(90)90452-Z

[4] Armentano, M, Dottori, E, Fortunati, S, Mattioli, J.M, Kenny, (2010). Biodegradable polymer matrix nanocomposites for tissue engineering, Polymer degradation and stability, **95**, pp. 2126-2146. http://dx.doi.org/10.1016/j.polymdegradstab.2010.06.007

[5] Barakat, M, Khil, M. S, Sheikhd, A, Kim, H.Y, (2009). Extraction of pure natural hydroxyapatite from the bovine bones bio waste by three different methods, Journal of materials processing technology, **209**, pp. 3408–3415. http://dx.doi.org/10.1016/j.jmatprotec.2008.07.040

[6] Ben-Nissan, B, (2003). Natural Bioceramics from coral to bone and beyond, Materials Science, **7**, pp. 283-288. http://dx.doi.org/10.1016/j.cossms.2003.10.001

[7] Boutinguiza, M, Pou, J, Comesana, R, Lusquinos, F, Carlos, A.D, Leon, B, (2012). Biological hydroxyapatite obtained from fish bones, Materials science and engineering, pp. 478-486. http://dx.doi.org/10.1016/j.msec.2011.11.021

[8] Braye, F, Irigaray, J.L, Jallot, E, Oudadesse, H, Weber, G, Deschamps, C, Deschamps, N, Frayss, P, Tourenne, P, Tixer, H, Terver, S, Lefaivre, J, Amirabadi, A, (1996). Ressorption kinetics of osseous substitute: natural coral and synthetic hydroxyapatite, Biomaterials, **17**, pp. 1345-1350. http://dx.doi.org/10.1016/0142-9612(96)88682-0

[9] Chattopadhyay, P, Pal, S, K, Singh, L and Verma, A, (2007). Synthesis of Crystalline Hydroxyapatite from Coral (Gergonaceasp) and Cytotoxicity Evaluation, Trends Biomatar. Artif. Organs, **20**, pp. 142-144.

[10] Clarke, A, Walsh, P, Maggs, C.A, (2011). Designs from the Deep Marine Organisms for Bone Tissue Engineering, Biotechnology Advances, 29, pp. 610–617. http://dx.doi.org/10.1016/j.biotechadv.2011.04.003

[11] Darimonta, G.L, Clootsb, R, Heinenc, E, Seideld, L, Legrand, R, (2002). In vivo behaviour of hydroxyapatite coatings on titanium implants: a quantitative study in the rabbit, Biomaterials, **23**, pp. 2569–2575. http://dx.doi.org/10.1016/S0142-9612(01)00392-1

[12] Descamps, M, Hornez, J.C, Leriche, A, (2009). Manufacture of Hydroxyapatite Beads for Medical Applications, Journal of the European Ceramic Society, **29**, pp. 369–375. http://dx.doi.org/10.1016/j.jeurceramsoc.2008.06.008

[13] Dorozhkin, S.V, (2013).A Detailed History of Calcium Orthophosphates from 1770s till 1950, Materials Science and Engineering, **33**, pp. 3085–3110. http://dx.doi.org/10.1016/j.msec.2013.04.002

[14] Dorozhkin, V.S, (2010). Calcium Orthophosphates as Bioceramics: State of the Art, Biomaterials, **1**, pp. 22-107.http://dx.doi.org/10.1016/j.biomaterials.2009.11.050

[15] Figueiredo, M, Fernando, A, Martins, G, Freitas, J, Judas, F, Figueiredo, H, (2010). Effect of the calcination temperature on the composition and microstructure of hydroxyapatite derived from human and animal bone, Ceramics International, **36**, pp. 2383-2393. http://dx.doi.org/10.1016/j.ceramint.2010.07.016

[16] Gergely, G, Weber, F, (2010). Preparation and Characterization of Hydroxyapatite from Eggshell, Ceramics International, **36**, pp. 803–806. http://dx.doi.org/10.1016/j.ceramint.2009.09.020

[17] Mehta, M.S, Singh, R.S, (2014). Effect of Aging Time and Sintering Temperatures on Structural, Morphological and Thermal Properties of Coralline Hydroxyapatite, IJRMET, **4**, pp. 2249-5762

[18] Nissan-Ben, B, Milev, A, Vago, R, (2004). Morphology of sol-gel derived nano-coated coralline hydroxyapatite, Biomaterials, **25**, pp. 4971-4975. http://dx.doi.org/10.1016/j.biomaterials.2004.02.006

[19] Oonishi, H, (1991). Orthopaedic applications of hydroxyapatite, Biomaterials, **12**, pp. 171-178. http://dx.doi.org/10.1016/0142-9612(91)90196-H

[20] Paitel, R.S, Narendra, B.D, (2009). Calcium phosphate coating for bio-implant ap plications:materials,performance factors,and methodologies,66, pp. 1-70.

[21] Yua, S, Hariramb, K.P, Kumara, R, Cheanga, P, Aik, K.K, (2005). In vitro apatite formation and its growth kinetics on hydroxyapatite/ polyetheretherketonebiocomposites, Biomaterials, **26**, pp. 2343–2352. http://dx.doi.org/10.1016/j.biomaterials.2004.07.028

[22] Zhou, H, Lee, Jaebeom, (2011). Nanoscale hydroxyapaitepaticles for bone tissue engineering, ActaBiomateriala, **7**, pp. 2769-2781.